

Full Length Research Paper

Preparative enrichment and separation of isofraxidin from *Acanthopanax senticosus* with HPD100C macroporous resin

Feng-jian Yang[#], Hong-shuang Ge[#], Lei Yang^{*}, Chun-jian Zhao, Wen-jie Wang, Ying Zhang, Lin Zhang and Yuan-gang Zu

Key Laboratory of Forest Plant Ecology, Ministry of Education, Northeast Forestry University, Harbin 150040, China.

Accepted 4 September, 2012

Isofraxidin is known as the major pharmacological component in *Acanthopanax senticosus*. In the present study, in order to screen a suitable resin for the preparative separation and purification of isofraxidin, the adsorption and desorption properties of 26 widely used commercial macroporous resins were evaluated. The preliminary research results indicated that HPD100C and HPD300 have better properties. By comparing static adsorption kinetics of HPD100C and HPD300, HPD100C was selected as the most suitable resin. Langmuir and Freundlich isotherms models were used to describe the interaction between solutes and resins at 25, 30, 35 °C, respectively, and the equilibrium experimental data fit better to the Langmuir isotherms. Dynamic adsorption and desorption tests have been carried out to optimize the process parameters. The optimal conditions were as follows: For adsorption, the concentration of isofraxidin in sample solution: 0.0436 mg/ml, processing volume: 24 BV, flow rate: 2 BV/h, temperature: 25 °C; for desorption, ethanol–water solution: 60:40 (v/v), eluent volume: 4 BV, flow rate: 3 BV/h. Under the conditions aforementioned, the content of isofraxidin increased 23.92-fold and its recovery was 93.79 ± 0.44%. In conclusion, HPD100C demonstrated the best ability for separating isofraxidin among the 26 tested resins.

Key words: *Acanthopanax senticosus*, macroporous resin, separation, isofraxidin.

INTRODUCTION

Radix *Acanthopanax senticosus* (RAS), is called "Siberian ginseng" or "*Eleutherococcus senticosus*", and has a name of Ciwujia in Chinese. It is the roots and rhizomes of *A. senticosus* that belongs to the Araliaceae family. RAS has been used extensively in China, Russia, Korea and Japan as an adaptogen (Brekhman and Dardymov, 1969; Davydov and Krikorian, 2000). Nowadays, there are some RAS products on the market of many countries, including drugs and healthy food (Davydov and Krikorian, 2000; Weng et al., 2007). In China, it is common for people using RAS to make medicinal liquor or to stew pigs,

milk cows and pigeons. *In vitro* and *in vivo* studies have demonstrated that RAS possesses many pharmacological effects, such as anti-stress, anti-fatigue, immuno-enhancing effect and anti-depressive effect, etc (Weng et al., 2007; Deyama et al., 2001). Among the active components in RAS and its extracts, isofraxidin (Figure 1) is the remarkable one and has been reported to possess strong biological activity (Zhang et al., 2002; Wang et al., 2003).

According to previous research results, isofraxidin is the major component attribute to the pharmacological effects of RAS. Isofraxidin was reported to exhibit anti-fatigue, anti-stress, and immuno-accomodating effects (Sun et al., 2007). Further investigations indicated that isofraxidin has the ability of diminishing inflammation (Yamazaki et al., 2004) and anbiosis (Liu et al., 2004a). Meanwhile, several studies have suggested that isofraxidin has anti-bacterial (Liu et al., 2004b) and anti-tumor effect

*Corresponding author. E-mail: ylnefu@163.com. Tel: +86-451-82191387. Fax: +86-451-82102082.

[#]Authors contributed equally to this work.

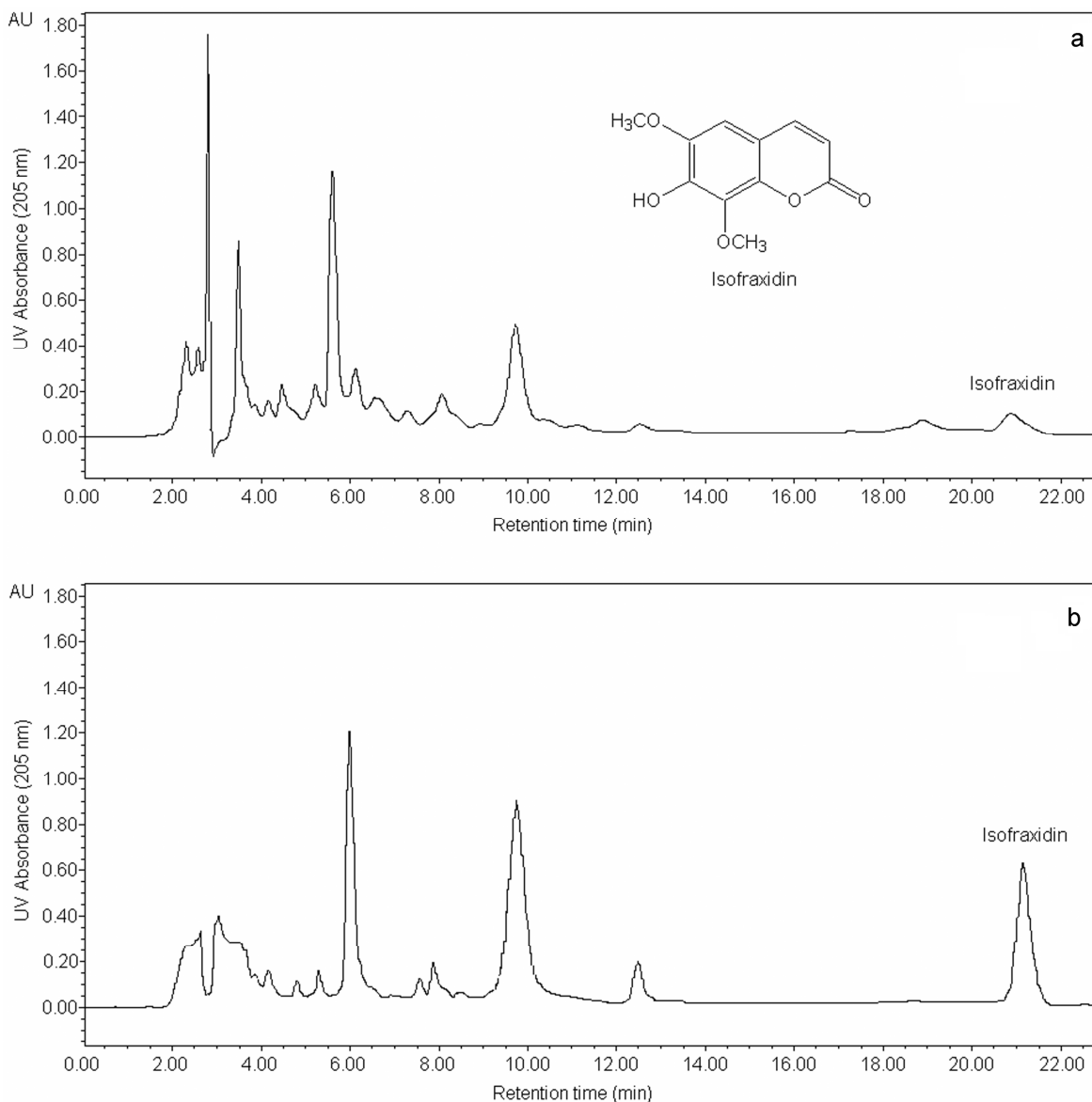


Figure 1. HPLC chromatograms of sample solution of *Acanthopanax senticosus* extracts (a) and desorption solution (b) from HPD100C. Inset: The molecular structure of isofraxidin.

(Yamazaki and Tokiwa, 2010). Due to the fact that natural isofraxidin has low content in RAS and the isolation was difficult, therefore, the development of an efficient separation method turns to be of extreme importance. Although, some methods have been used to separate isofraxidin from RAS, such as liquid–liquid partition (Méndez, 1978; Yang et al., 2010), column chromatographic procedures involving cellulose (Méndez, 1978) and high-speed counter-current chromatography (Xiao et al., 2009) etc.

However, due to their relative low handling capacity in one cycle, these separation methods are inefficient. They are also troubled with various other disadvantages, such as low recovery, large solvent consuming, high labor

intensities and operation cost, or even safety problems. Those deficits make them unsuitable for large-scale industrial production (Fu et al., 2006; Jia and Lu, 2008). As a kind of adsorbent, macroporous resin can be used to selectively adsorb constituents from aqueous solution through hydrogen bonding forces and van der Waals forces, etc (Pi et al., 2008; Jiang et al., 2006; Gao et al., 2007). The adsorption–desorption process by macroporous resins, as an efficient separation method, usually shows a high adsorption, easy desorption, low costs of operation and easy regeneration (Liu et al., 2004, 2012; Jin et al., 2008; Silva et al., 2007). Furthermore, it has been an ever growing research to separate pharmacological components from herbal materials

employing macroporous resins (Jia and Lu, 2008; Fu et al., 2005, 2007; Mi and Song, 2001; Drasar and Moravcova, 2004; Liu et al., 2008; Ma et al., 2011).

Moreover, in the previous study (He et al., 2007), 12-1 macroporous resin was tested for the separation of isofraxidin from *Sarcandra glabra* extract, the resin was not optimized and the adsorption capacity was not satisfactory, the parameters for static adsorption and desorption tests were not optimized. Thus, in this study, we have focused on investigating the adsorption and desorption properties of 26 different resins on separating and purifying isofraxidin from RAS. Then, based on the experimental results, the most suitable resin was selected and used to develop an efficient and simple method of separating and purifying isofraxidin in large scale from RAS.

MATERIALS AND METHODS

Chemical and reagents

Radix *Acanthopanax senticosus* (RAS) was obtained from Sankeshu Medicinal Materials Market (Harbin, China), and was minced into little pieces and sieved through 20 to 40 meshes before use. Isofraxidin standard (95% purity) was purchased from National Institute for the Control of Pharmaceutical and Biological Products (Beijing, China). Acetonitrile of chromatographic grade was purchased from J and K Chemical Limited (Beijing, China). Deionized water was freshly prepared by a Milli-Q water-purification system (Millipore, Bedford, MA, USA) and used in all experiments. Other reagents are analytical grade and were purchased from Beijing Chemical Reagents Co. (Beijing, China). All solvents prepared for HPLC were filtered through 0.45 μm nylon membrane and degassed under ultrasonication before use.

Adsorbents

Macroporous resins tested were purchased from Cangzhou Bon Adsorber Technology Company Limited (Cangzhou, China). Their physical properties are listed in Table 1. In order to remove the monomers and porogenic agents trapped inside the pores of macroporous resin during synthesis process, the adsorbent beads were pretreated with the following procedure: first, the resins were soaked in ethanol for 24 h, and then washed with deionized water by circumfluence until there is no residue of ethanol. The treated resins were stored in a desiccator with deionized water in order to maintain constant moisture content. Prior to use, the resins were wet with ethanol again and then thoroughly replaced with deionized water (Apers et al., 2005; Jung et al., 2001). In order to obtain moisture contents of macroporous resins, the resins were accurately weighed in glass dishes, and dried to a constant weight in a digital blast oven (Shanghai Boxun Industry and Commerce Co., Ltd., Shanghai, China) at 105°C. Their moisture contents were calculated and were also shown in Table 1.

HPLC analysis of isofraxidin

A waters liquid chromatograph (Waters Corporation, Milford, MA, USA), consisting of a Waters 600 Controller equipped with a Waters 717 plus autosampler, and a Waters 2487 UV detector was used to determine isofraxidin. Chromatographic separation was carried out on a Kromasil C18 reversed-phase column (5 μm diameter

particles, 4.6 mm \times 250 mm I.D., Kromasil). The mobile phase was acetonitrile–water–formic acid (15:84.9:0.1, v/v/v). The detection wavelength was 205 nm, the flow rate was 1 ml/min, the injection volume was 10 μL , and the column temperature was maintained at 25°C. The regression line for isofraxidin was $Y = 20021348X - 139160$ ($R^2 = 0.9993$, $n = 8$), where Y was the peak area of isofraxidin and X was the concentration of isofraxidin (mg/ml).

Preparation of crude RAS extracts

The minced RAS powder (2000 g) was extracted with deionized water (12 L) under reflux for 30 min each time, repeated three times. The extract solution was purified by membrane filtration and then evaporated in rotary vaporization (RAS-52AA, Shanghai Huxi Instrument, and Shanghai, China) to dryness under vacuum condition. The dry extract was stored at 4°C. The contents of isofraxidin in the extract were 0.0533%.

Static adsorption and desorption properties of the resins

The static adsorption tests of RAS extract were performed as follows: 0.5 g resins (dry weight basis) were added into a conical flask with a lid and then 100 ml aqueous sample solutions with known concentrations prepared in section 2.3 were introduced. The flasks were then shaken (100 rpm) for 8 h at 25°C in a constant temperature oscillator (Harbin Donglian Electronic and Technology Development Company Limited Harbin, China). The initial concentration of sample solutions and their concentrations post adsorption were analyzed by HPLC.

The static desorption process was carried out as follows: after reaching adsorption equilibrium, the residual solution was removed. The adsorbate-laden resins were first washed in 100 ml deionized water, shaken (100 rpm) for 2 h at 25°C. Then, they were desorbed in 25 ml ethanol-water (95:5, v/v) solution. The flasks were shaken (100 rpm) for 2 h at 25°C. Desorption solutions were also analyzed by HPLC. The suitable resin was selected based on its adsorption capacity and desorption ratio.

Static adsorption kinetics on HPD100C and HPD300

The static adsorption kinetics of isofraxidin on the preliminarily selected resins, HPD100C and HPD300, were also studied using the same procedure as previously described. The respective concentrations of isofraxidin in the sample solutions were monitored by HPLC at predetermined time intervals until equilibrium.

Adsorption isotherms

The adsorption isotherm of isofraxidin on the optimum resin, HPD100C was investigated by contacting 100 ml of sample solutions at different concentrations with pre-weighed resins 0.5 g (dry weight basis) in the shaker bath (100 rpm) for 8 h at 25, 30 and 35°C. The initial and equilibrium concentrations were determined by HPLC. The equilibrium adsorption isotherm on the resin was obtained, and their degrees of fitness to the Langmuir equation and Freundlich equation were evaluated.

Dynamic adsorption and desorption

Dynamic adsorption and desorption experiments were carried out in a glass columns (12 mm \times 500 mm) (Tianjin Tianbo Glass Instrument Co., Ltd., Tianjin, China) wet-packed with 5 g (dry weight

Table 1. Physical properties and absorption characteristics of the test macro-porous resins.

Resin	Surface area (m ² /g)	Average pore diameter (Å)	Particle diameter (mm)	Polarity	Moisture content (%)	Adsorption capacity (mg/g)	Desorption ratio (%)
HPD80	350-400	80-85	0.30-1.25	Non-polar	67.84	0.86 ± 0.04	55.08 ± 2.26
HPD100	650-700	85-90	0.30-1.20	Non-polar	65.00	4.59 ± 0.23	44.03 ± 2.19
HPD100A	650-700	95-100	0.30-1.20	Non-polar	66.67	3.06 ± 0.15	38.17 ± 1.86
HPD100B	500-580	120-160	0.30-1.25	Non-polar	61.49	3.96 ± 0.20	45.55 ± 2.25
HPD100C	720-760	80-90	0.30-1.25	Non-polar	61.68	4.76 ± 0.19	82.01 ± 3.11
HPD200A	700-750	85-90	0.30-1.25	Non-polar	54.90	4.02 ± 0.20	48.58 ± 2.29
HPD300	800-870	50-55	0.30-1.20	Non-polar	75.52	4.75 ± 0.20	57.15 ± 2.90
HPD700	650-700	85-90	0.30-1.20	Non-polar	66.10	4.25 ± 0.21	42.27 ± 2.19
HPDD	650-750	90-110	0.30-1.25	Non-polar	73.06	3.21 ± 0.16	51.98 ± 2.57
D101	≥400	100-110	0.30-1.25	Non-polar	66.47	3.23 ± 0.16	52.67 ± 2.49
HPD910	450-550	85-90	0.30-1.25	Non-polar	50.00	2.52 ± 0.13	66.57 ± 3.25
HPD722	485-530	130-140	0.30-1.25	Weak-polar	58.95	0.20 ± 0.01	-
AB-8	480-520	130-140	0.30-1.25	Weak-polar	65.00	3.23 ± 0.16	33.43 ± 1.46
HPD450	500-550	90-110	0.30-1.20	Weak-polar	72.00	3.41 ± 0.17	44.53 ± 2.53
HPD450A	500-550	90-100	0.30-1.25	Middle-polar	72.37	2.79 ± 0.14	78.46 ± 3.90
HPD400A	500-550	85-90	0.30-1.20	Middle-polar	64.06	3.21 ± 0.17	42.88 ± 2.06
HPD750	650-700	85-90	0.30-1.20	Middle-polar	57.58	3.44 ± 0.17	41.86 ± 2.23
HPD850	1100-1300	85-95	0.30-1.20	Middle-polar	46.81	3.22 ± 0.16	56.74 ± 2.76
DM130	500-550	90-100	0.30-1.25	Middle-polar	66.48	2.60 ± 0.13	52.74 ± 2.63
HPD400	500-550	75-80	0.30-1.20	Polar	68.93	4.33 ± 0.22	43.39 ± 2.23
HPD500	500-550	55-75	0.30-1.20	Polar	70.45	3.44 ± 0.17	61.27 ± 3.12
HPD600	550-600	80	0.30-1.20	Polar	69.32	3.95 ± 0.20	52.11 ± 2.57
ADS-7	≥100	250-300	0.30-1.25	Polar	63.23	2.80 ± 0.14	46.11 ± 2.19
ADS-17	90-150	250-300	0.30-1.25	Hydrogen-bonding	51.06	1.25 ± 0.06	45.59 ± 2.33
HPD417	90-150	250-300	0.30-1.25	Hydrogen-bonding	54.55	2.02 ± 0.10	31.23 ± 1.24
HPD826	500-600	90-100	0.30-1.25	Hydrogen-bonding	67.52	4.00 ± 0.20	52.75 ± 2.46

where mean ± S.D., n=3; “-” indicates that there is no signal in HPLC profiles.

basis) HPD100C. The bed volume (BV) and the length of the resin were 25 ml and 10 cm, respectively. In all cases, the sample solutions were flowed downward. Sample solutions were flowed through the glass column at certain flow rate, and the isofraxidin concentration was monitored by HPLC analysis of the effluent liquid collected at 50 ml intervals. Breakthrough point was indicated. Once adsorption reached equilibrium, the loading of the sample

solution was stopped. The adsorbate-laden columns were first washed with deionized water and then with different ethanol-water solutions (30:70, 40:60, 50:50, 60:40, 70:30, 80:20, 90:10, v/v), at the same flow rate. The isofraxidin concentration in the effluent solution was determined by HPLC analysis of the effluent liquid collected at 5 ml intervals. The effluent solution were concentrated and dried under vacuum before further analyses. The dynamic

adsorption and desorption capacities of HPD100C, the recoveries and the isofraxidin content in the product were calculated.

Dynamic adsorption and desorption capacity, the recovery equation

The following equations were used to quantify the adsorption

and desorption capacity and the desorption ratio as well as the recovery. Adsorption evaluation is calculated as:

$$Q_e = (C_0 - C_e) \cdot \frac{V_i}{W} \quad (1)$$

where Q_e is the adsorption capacity at adsorption equilibrium (mg/g resin); C_0 and C_e are the initial and equilibrium concentration of isofraxidin in the solutions (mg/ml); V_i is the volume of the initial sample solution (ml) and W is the weight of the dry resin (g). Desorption evaluation is calculated as:

$$D = \frac{C_d \cdot V_d}{(C_0 - C_e) \cdot V_i} \cdot 100\% \quad (2)$$

$$Q_d = \frac{C_d \cdot V_d}{W} \quad (3)$$

Where D is the desorption ratio (%); Q_d is the desorption capacity after adsorption equilibrium (mg/g resin); C_d is the isofraxidin concentration in the desorption effluent solutions (mg/mL); V_d is the volume of the desorption solutions; C_0 , C_e , V_i and W are the same as those defined in Equation (1). The following equation was used to calculate the recovery.

$$R = \frac{m}{M} \cdot 100\% \quad (4)$$

where R is the recovery (%), M is the weight of a targeted component laden onto the selected adsorbent; m is the weight of the targeted component in product.

Langmuir equation and Freundlich equation

The equilibrium experimental data were fitted to the Langmuir and Freundlich isotherms equations (Fu et al., 2007, 2008; Jung et al., 2001) to describe the adsorption behavior between solute and resin. The Langmuir isotherms equation is given as:

$$\frac{C_e}{Q_e} = \frac{C_e}{Q_{\max}} + \frac{1}{k \cdot Q_{\max}} \quad (5)$$

The aforementioned equation can be rearranged to the following linear form:

$$\frac{1}{Q_e} = \frac{1}{K_L \cdot C_e} + \frac{1}{Q_{\max}} \quad (6)$$

Where Q_{\max} is the theoretically calculated maximum adsorption capacity (mg/g resin); k and K_L are constant; Q_e is the adsorption capacity at adsorption equilibrium (mg/g resin) and C_e is the equilibrium concentrations of solutes in the solutions. The Freundlich isotherms equation is given as:

$$Q_e = K_F \cdot C_e^{1/n} \quad (7)$$

A linearized form of Equation (7) can be written as:

$$\log Q_e = \log K_F + \left(\frac{1}{n}\right) \cdot \log C_e \quad (8)$$

where K_F is constant, an indicator of adsorption capacity; $1/n$ is an empirical constant related to the magnitude of the adsorption driving force; Q_e and C_e are the same as those defined in Equations (5) and (6).

RESULTS AND DISCUSSION

Adsorption and desorption properties of the resins

As shown in Table 1, the adsorption and desorption properties of different resins are distinct. The adsorption capacities of HPD100C and HPD300 were higher than those of other resins. In general, the adsorption capacity of a resin is correlated with its surface area. HPD100C and HPD300 have larger surface area than other resins, which may account for their higher adsorption capacity for isofraxidin. Therefore, due to their high surface area and similar polarity with isofraxidin, HPD100C and HPD300 owned better adsorption capacity.

On the other hand, HPD100C and HPD300 also showed higher desorption capacity and desorption ratio for isofraxidin than others. It may be due to the fact that the affinity between isofraxidin and resin is mainly the physical force, such as the van der Waals force, which has a low power for holding the isofraxidin on HPD100C and HPD300. Moreover, even though a big average pore diameter may bring in high desorption ratio, they also incur low adsorption and desorption capacity. Thus, due to the affinity and the proper average pore diameter, HPD100C and HPD300 had better desorption capacity and desorption ratio.

In addition, the ranking in Table 1 appears to reflect the different physicochemical properties of these resins. Compared with other resins, HPD100C and HPD300 owned better adsorption and desorption capacity and higher desorption ratio for isofraxidin. Therefore, HPD100C and HPD300 were selected for further study in the following adsorption kinetics experiments.

Static adsorption kinetics on HPD100C and HPD300

The static adsorption and desorption experiments are not enough for evaluating the performance of an adsorbent. A more suitable resin must also have a higher adsorption rate. Therefore, the adsorption kinetics curves were obtained for isofraxidin on HPD100C and HPD300. As can be seen in Figure 2, the adsorption capacity increased with the increasing of the adsorption time, reaching equilibrium at about 3 h on HPD100C and 4 h on HPD300, respectively. In Figure 2, it is apparent that HPD100C has a better adsorption rate than HPD300. Thus, HPD100C was selected for further study in the following tests.

Adsorption isotherms

The adsorption isotherms of HPD100C were investigated

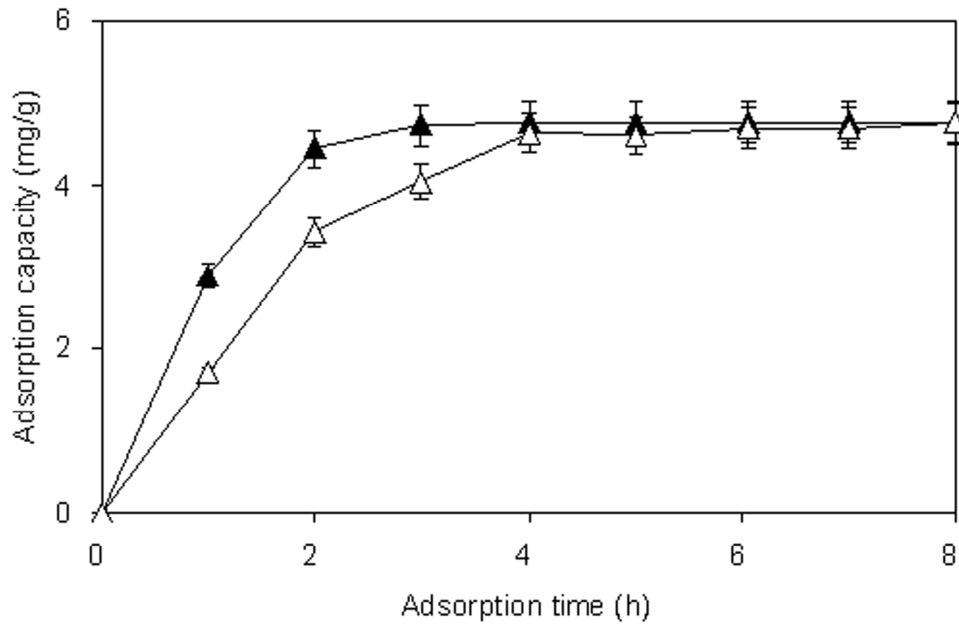


Figure 2. Adsorption kinetics curves for isofraxidin on HPD100C and HPD300.

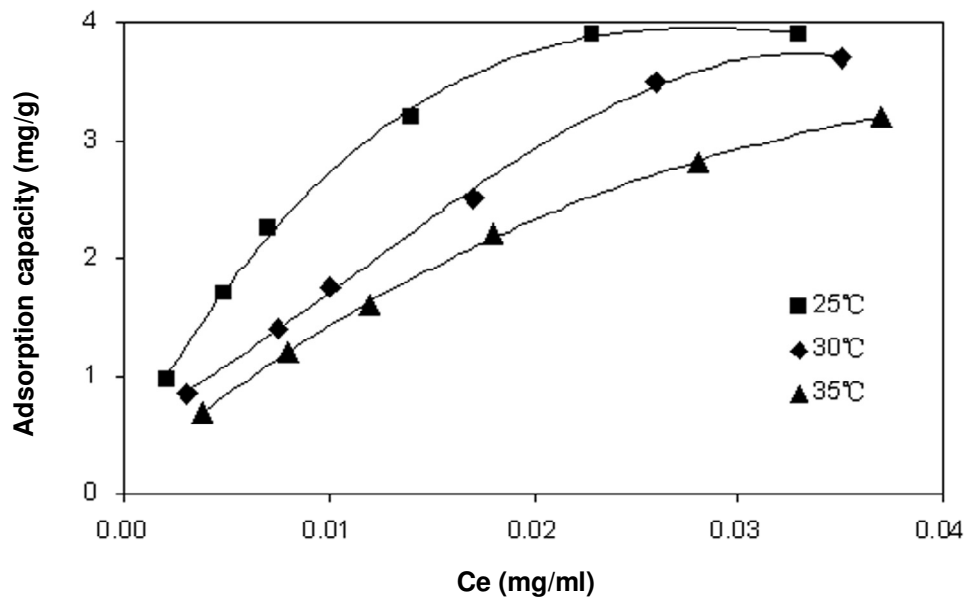


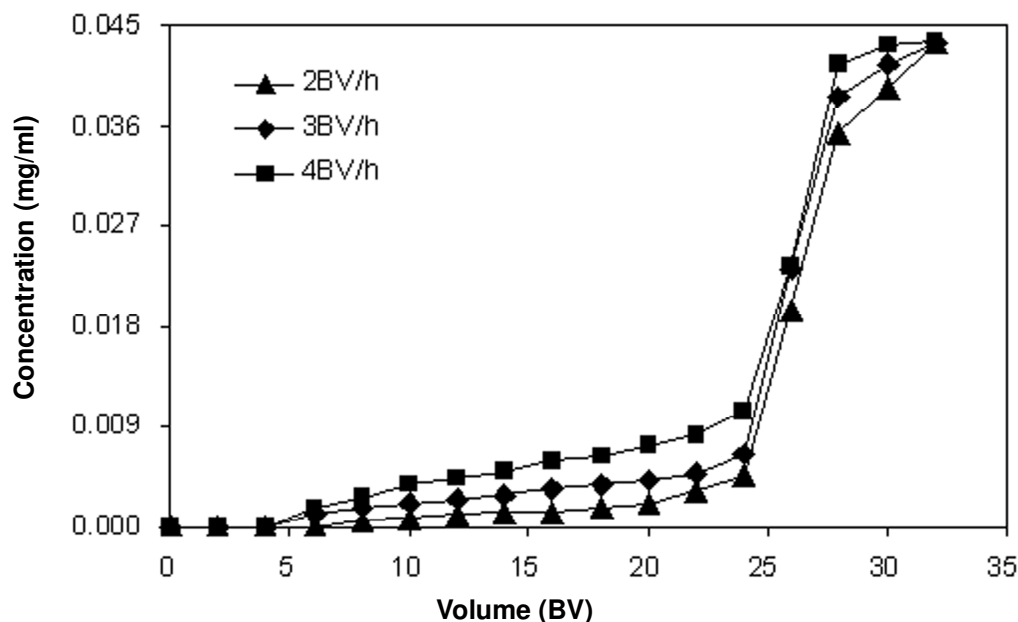
Figure 3. Adsorption isotherm at 25, 30 and 35°C for isofraxidin on HPD100C.

with different concentrations of sample solutions at 25, 30, 35°C. The initial concentrations of isofraxidin were 0.0077, 0.0144, 0.0190, 0.0297, 0.0436 and 0.0537 mg/ml, respectively. As shown in Figure 3, the adsorption capacities increased with the increasing of the initial solute concentrations, and reached the saturation plateau when the initial concentration of isofraxidin was 0.0436 mg/ml.

Equilibrium data gives information about the affinity between solute and adsorbent. The Langmuir isotherm model and the Freundlich isotherm model are the two best-known and the most often-used isotherms model for the adsorption of solute from solution. The Langmuir and Freundlich parameters are summarized in Table 2. As can be seen in Table 2, for Freundlich equation, the adsorption can easily take place when $1/n$ value is

Table 2. Langmuir and Freundlich parameters of isofraxidin on HPC100C at 25, 30 and 35°C.

Temperature (°C)	Langmuir equation			Freundlich equation		
	Q_{max}	K_L	R^2	K_F	n	R^2
25	6.33	434.78	0.9972	35.1965	1.7015	0.9622
30	5.42	289.02	0.9857	38.9404	1.4943	0.9903
35	4.79	208.33	0.9821	33.7054	1.4347	0.9942

**Figure 4.** Dynamic leakage curves of isofraxidin on column packed with HPD100C.

between 0.1 and 0.5 and tends not to happen when $1/n$ value is between 0.5 and 1, and is almost unable to occur when $1/n$ value exceeds 1 (Liu et al., 2008). In isofraxidin's Freundlich equation, all $1/n$ values are between 0.5 and 1. Thus, even though the R^2 values of isofraxidin's Freundlich equation were rather high, it is hard for the adsorption of isofraxidin on HPD100C to happen. On the other hand, the R^2 values of isofraxidin's Langmuir equation were all above 0.98. Thus, the Langmuir equation can describe the adsorption and desorption behavior of isofraxidin on HPC100C.

Langmuir isotherm model is based on the assumption that the sorbate form is only a single layer (Campbell and Davies, 1995), thus, the results in Table 2 showed that it is the single layer form adsorption between particles of isofraxidin and the surface of HPD100C. As shown in Figure 3, at the same initial concentration, the adsorption capacities decreased with the increasing of the temperature in the investigated temperature range, which indicated that the adsorption was a thermo positive process. Meanwhile, Q_{max} also decreased with increasing temperature for isofraxidin (Table 2). Therefore, 25°C was

selected in the following experiments.

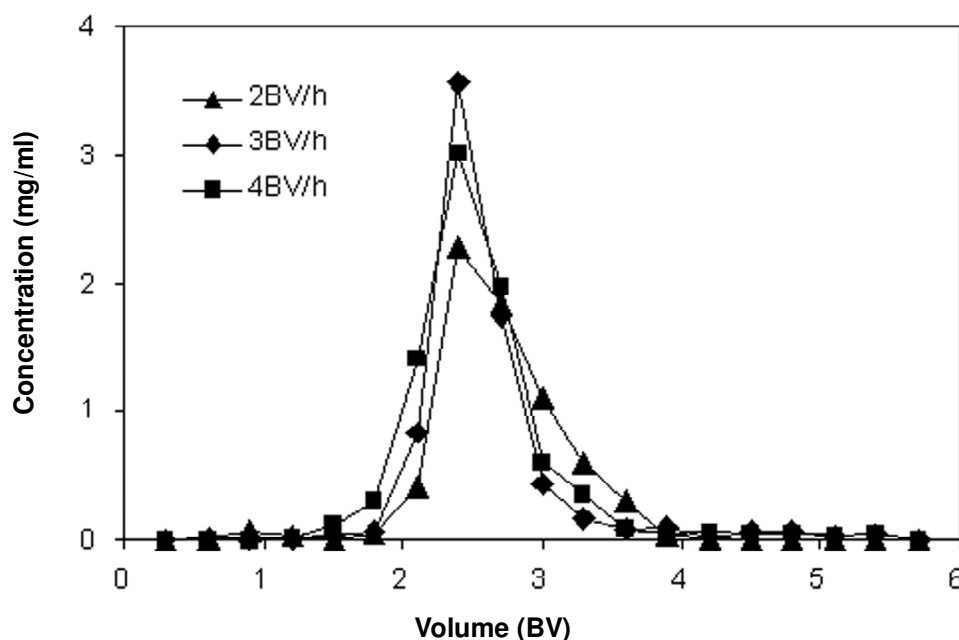
Dynamic leakage curves on HPD-100C resin

The initial concentration of isofraxidin in this test was 0.0436 mg/ml, and the flow rates investigated in this test were 2, 3 and 4 BV/h, respectively. The dynamic leakage curves on HPD-100C resin were obtained based on the effluent volume and the concentration of solute in sample solution. As can be seen in Figure 4, the isofraxidin exhibited better adsorption performance at the flow rate of 2 BV/h, this may be due to a better particle diffusion in sample solution. Therefore, 2 BV/h was selected in the following tests. For breakthrough point, when the concentration in leak solution is 10% of the initial concentration, adsorption is presumed to have reached saturation, when the adsorption affinity decreases, or even disappears, and then the solutes leak from the resin. Thus, breakthrough point is usually defined as the time when the leak solution concentration is equal to 10% of the initial concentration. It is important to set up the

Table 3. Effects of different ethanol-water solution as desorption solutions on desorption properties of HPD100C for isofraxidin.

Ethanol-water solution (v/v)	30:70	40:60	50:50	60:40	70:30	80:20	90:10
Mass of dried residue (g)	2.00 ± 0.09	2.06 ± 0.11	2.09 ± 0.11	2.17 ± 0.10	2.38 ± 0.12	2.83 ± 0.10	3.50 ± 0.12
Mass of isofraxidin (mg)	12.54 ± 0.58	14.21 ± 0.73	21.18 ± 1.12	27.62 ± 1.39	27.71 ± 1.38	27.82 ± 1.42	27.98 ± 1.42
Content of isofraxidin (%)	0.63 ± 0.03	0.69 ± 0.03	1.01 ± 0.05	1.28 ± 0.06	1.16 ± 0.06	0.98 ± 0.05	0.80 ± 0.04

where mean ± S.D., n=3.

**Figure 5.** Dynamic desorption curves of isofraxidin on a column packed with HPD100C.

leakage curve. In the present case, the breakthrough point of isofraxidin appeared at a processing volume of sample solution around 24 BV.

Effect of ethanol-water solution on desorption tests

In order to choose proper desorption solution, different ethanol-water solutions (30:70, 40:60, 50:50, 60:40, 70:30, 80:20, 90:10, v/v) were used to perform desorption tests. As can be seen in Table 3, on one hand, with the increase of the ethanol-water solution, the desorption mass of isofraxidin has increased markedly until the ethanol-water solution reaches 60:40 (v/v), and raised slightly passing this point; on the other hand, the desorption contents of isofraxidin gradually increased and reached their peak value at the ethanol-water (60:40, v/v) solution, and then decreased. When ethanol-water solution exceeds 60:40 (v/v), the desorbed impurities also increased. At the ethanol-water (60:40, v/v) solution, desorption mass of isofraxidin was 27.62 mg, and the relative content was the highest comparing with those at

other ethanol-water solutions. Thus, ethanol-water (60:40, v/v) solution was selected as the appropriate desorption solution and used in the following dynamic desorption experiments.

Dynamic desorption curve on HPD100C

The ethanol-water (60:40, v/v) solution was used to elute isofraxidin. The flow rates investigated in this test were 2, 3 and 4 BV/h, respectively. The dynamic desorption curves on HPD100C were obtained based on the volume of desorption solution and the concentration of solute. As can be seen in Figure 5, the isofraxidin exhibited better desorption performance at the flow rate of 3 BV/h. At this flow rate, isofraxidin was thoroughly desorbed in 3.5 BV. The results indicated that the process of 3 BV/h reduces ethanol solutions used and shortens the desorption process. Therefore, 3 BV/h was selected as the proper desorption flow rate considering its lower volume consumption and high efficiency.

The optimum parameters for the preparative separation

of isofraxidin on HPD100C were confirmed as follows: for adsorption, the concentration of isofraxidin in sample solution: 0.0436 mg/ml, processing volume: 24 BV, flow rate: 2 BV/h, temperature: 25°C; for desorption, ethanol-water solution: 60:40 (v/v), eluent volume: 4 BV, flow rate: 3 BV/h.

The HPLC profiles of the samples before and after HPD100C chromatography are shown in Figure 1. By comparison, it can be seen that some impurities were removed from the sample solution and the relative peak area of isofraxidin increased pronouncedly after the separation treatment on HPD100C. The eluate was obtained under the optimum conditions, and freeze-dried after the ethanol was removed. After the separation on HPD100C resin, the content of isofraxidin increased 23.92-fold from 0.0533 ± 0.0004 to $1.2752 \pm 0.0077\%$ and the recovery rate was $93.79 \pm 0.44\%$.

Conclusions

In this study, the preparative separation of isofraxidin from RAS using macroporous resin was successfully achieved, and was demonstrated to be an approach with broad prospect. Among the 26 resins tested, HPD100C was selected due to its higher surface area, optimum average pore diameter, appropriate surface functional polarity, and its absorption power resulted from the hydrogen bonding and van der Waals forces.

The equilibrium adsorption experiment at 25°C on HPD100C was fitted to the Langmuir isotherms model. In addition, the processes of dynamic adsorption and desorption were conducted to achieve the optimal separation parameters. Through the treatment on a column packed with HPD100C, the optimal adsorption and desorption conditions about simultaneous separation of isofraxidin from RAS were obtained. After the treatment on HPD100C, the content of isofraxidin improved 23.92-fold. The recovery was $93.79 \pm 0.44\%$.

ACKNOWLEDGEMENTS

The authors gratefully acknowledge the financial support by National Key Technology Research and Development Program (2011BAD33B0203).

REFERENCES

- Apers S, Naessens T, van Miert S, Pieters L, Vlietinck A (2005). Quality control of roots of *Eleutherococcus senticosus* by HPLC. *Phytochem. Anal.* 16:55-60.
- Brekhman II, Dardymov IV (1969). New substances of plant origin which increase nonspecific resistance. *Annu. Rev. Pharmacol.* 9:419-430.
- Campbell LS, Davies BE (1995). Soil sorption of caesium modelled by the Langmuir and Freundlich isotherm equations. *Appl. Geochem.* 10:715-723.
- Davydov M, Krikorian AD (2000). *Eleutherococcus senticosus* (Rupr. & Maxim.) Maxim. (Araliaceae) as an adaptogen: a closer look. *J. Ethnopharmacol.* 72:345-393.
- Deyama T, Nishibe S, Nakazawa Y (2001). Constituents and pharmacological effects of *Eucommia* and Siberian ginseng. *Acta Pharmacol. Sin.* 22:1057-1070.
- Drasar P, Moravcova J (2004). Recent advances in analysis of Chinese medical plants and traditional medicines. *J. Chromatogr. B* 812:3-21.
- Fu B, Liu J, Li H, Li L, Lee FS, Wang X (2005). The application of macroporous resins in the separation of licorice flavonoids and glycyrrhizic acid. *J. Chromatogr. A* 1089:18-24.
- Fu Y, Zu Y, Li S, Sun R, Efferth T, Liu W, Jiang S, Luo H, Wang Y (2008). Separation of 7-xylosyl-10-deacetyl paclitaxel and 10-deacetyl baccatin III from the remainder extracts free of paclitaxel using macroporous resins. *J. Chromatogr. A* 1177:77-86.
- Fu Y, Zu Y, Liu W, Efferth T, Zhang N, Liu X, Kong Y (2006). Optimization of luteolin separation from pigeonpea [*Cajanus cajan* (L.) Millsp.] leaves by macroporous resins. *J. Chromatogr. A* 1137:145-152.
- Fu Y, Zu Y, Liu W, Hou C, Chen L, Li S, Shi X, Tong M (2007). Preparative separation of vitexin and isovitexin from pigeonpea extracts with macroporous resins. *J. Chromatogr. A* 1139:206-213.
- Gao M, Huang W, Liu CZ (2007). Separation of scutellarin from crude extracts of *Erigeron breviscapus* (vant.) Hand. Mazz. by macroporous resins. *J. Chromatogr. B* 858:22-26.
- He XZ, Xu GL, Xiao BH, Chen Q (2007). Quality evaluation of isofraxidin part in *Sarcandra glabra* extract separated by macroporous adsorptive resin. *J. Jiangxi University TCM* 19:45-46.
- Jia G, Lu X (2008). Enrichment and purification of madecassoside and asiaticoside from *Centella asiatica* extracts with macroporous resins. *J. Chromatogr. A* 1193:136-141.
- Jiang X, Zhou J, Zhou C (2006). Study on adsorption and separation of naringin with macroporous resin. *Frontiers of Chemistry in China* 1:77-81.
- Jin Q, Yue J, Shan L, Tao G, Wang X, Qiu A (2008). Process research of macroporous resin chromatography for separation of N-(p-coumaroyl)serotonin and N-feruloylserotonin from Chinese safflower seed extracts. *Sep. Purif. Technol.* 62:370-375.
- Jung MW, Ahn KH, Lee Y, Kim KP, Paeng IR, Rhee JS, Park JT, Paeng KJ (2001). Evaluation on the adsorption capabilities of new chemically modified polymeric adsorbents with protoporphyrin IX. *J. Chromatogr. A* 917:87-93.
- Liu J, Tian J, Hu Z, Chen X (2004a). Binding of isofraxidin to bovine serum albumin. *Biopolymers* 73:443-450.
- Liu J, Tian J, Tian X, Hu Z, Chen X (2004b). Interaction of isofraxidin with human serum albumin. *Bioorg. Med. Chem.* 12:469-474.
- Liu T, Ma C, Sui X, Yang L, Zu Y (2012). Preparation of shikonin by hydrolyzing ester derivatives using basic anion ion exchange resin as solid catalyst. *Ind. Crops Products* 36:47-53.
- Liu S, Yi L, Liang Y (2008). Traditional Chinese medicine and separation science. *J. Sep. Sci.* 31:2113-2137.
- Liu X, Xiao G, Chen W, Xu Y, Wu J (2004). Quantification and purification of mulberry anthocyanins with macroporous resins. *J. Biomed. Biotechnol.* 5:326-331.
- Ma C, Liu T, Yang L, Zu Y, Yang F, Zhao C, Zhang L, Zhang Z (2011). Preparation of high purity biphenyl cyclooctene lignans from *Schisandra* extract by ion exchange resin catalytic transformation combined with macroporous resin separation. *J. Chromatogr. B* 30:3444-3451.
- Méndez J (1978). Isofraxidin in *Erica* flowers. *Phytochemistry*. 17:820.
- Mi J, Song C (2001). Advances of application of macroporous resin in study of traditional Chinese herbs. *Chin. Trad. Patent Med.* 23:914-917.
- Pi G, Ren P, Yu J, Shi R, Yuan Z, Wang C (2008). Separation of sanguinarine and chelerythrine in *Macleaya cordata* (Willd) R. Br. based on methyl acrylate-co-divinylbenzene macroporous adsorbents. *J. Chromatogr. A* 1192:17-24.
- Silva EM, Pompeu DR, Larondelle Y, Rogez H (2007). Optimisation of the adsorption of polyphenols from *Inga edulis* leaves on macroporous resins using an experimental design methodology. *Sep. Purif. Technol.* 53:274-280.
- Sun H, Lü HT, Zhang YM, Wang XJ, Bi KS, Cao HX (2007). Pharmacokinetics of isofraxidin in rat plasma after oral administration of the extract of *Acanthopanax senticosus* using HPLC with solid phase extraction method. *Chem. Pharm. Bull.* 55:1291-1295.

- Weng S, Tang J, Wang G, Wang X, Wang H (2007). Comparison of the addition of Siberian ginseng (*Acanthopanax senticosus*) versus fluoxetine to lithium for the treatment of bipolar disorder in adolescents: a randomized, double-blind trial. *Curr. Ther. Res.* 68:280-290.
- Wang ZY, Lin JM, Zhang ZY (2003). Chemical constituents and pharmacology of *Acanthopanax senticosus*. *J. Chin. Med. Mat.* 26:603-606.
- Xiao XH, Guo ZN, Deng JC, Li GK (2009). Separation and purification of isofraxidin from *Sarcandra glabra* by microwave-assisted extraction coupled with high-speed counter-current chromatography. *Sep. Purif. Technol.* 68:250-254.
- Yamazaki T, Tokiwa T, Shimosaka S, Sakurai M, Matsumura T, Tsukiyama T (2004). Anti-inflammatory effects of a major component of *Acanthopanax senticosus* Harms, isofraxidin. *J. Electrophor.* 48:55-58.
- Yamazaki T, Tokiwa T (2010). Isofraxidin, a coumarin component from *Acanthopanax senticosus*, inhibits matrix metalloproteinase-7 expression and cell invasion of human hepatoma cells. *Biol. Pharm. Bull.* 33:1716-1722.
- Yang L, Hao JW, Liu Y, Liu TT, Zu YG (2010). Isolated isofraxidin from *Acanthopanax senticosus* extract by extraction in combination hydrolysis in situ. *Chin. J. Modern Appl. Pharm.* 27:401-405.
- Zhang Y, Liu BZ, Pei YH (2002). Pharmacological action of *Acanthopanax senticosus* (Rupr. et Maxim.) Harms. *J. Shenyang Pharm. Univ.* 19:143-146